Chemical Science

Accepted Manuscript

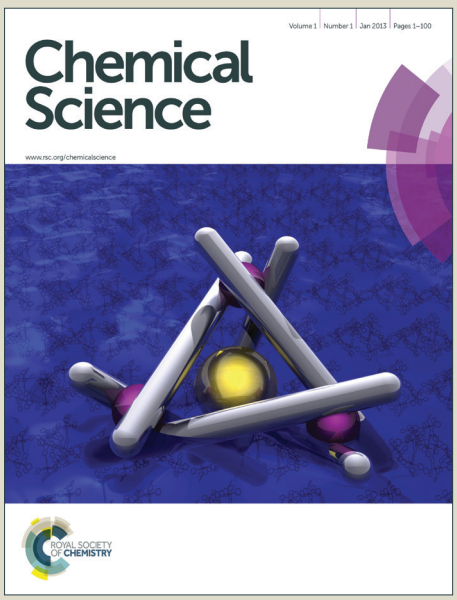

ROYAL SOCIETY OF CHEMISTRY

www.rsc.org/chemicalscience

Cite this: DOI: 10.1039/c0xx00000x

www.rsc.org/xxxxxx

ARTICLE TYPE

A sialic acid-targeted near-infrared theranostic for signal activation based intraoperative tumor ablation

Xuanjun Wu,[a] Mingzhu Yu,[a] Bijuan Lin,[a] Hongjie Xing,[a] Jiahuai Han,[b] and Shoufa Han[a,*]

Received (in XXX, XXX) Xth XXXXXXXXX 20XX, Accepted Xth XXXXXXXXX 20XX

DOI: 10.1039/b000000x

Agents enabling tumor staging are valuable for cancer surgery. Herein a targetable sialic acid-armed near-infrared profluorophore (SA-pNIR) is reported for fluorescence guided tumor detection. SA-pNIR consists of a sialic acid entity effective for *in vivo* tumor-targeting and a proflurophore which undergoes lysosomal acidity triggered fluorogenic isomerization. SA-pNIR displays a number of advantageous biomedical properties in mice, *e.g.* high tumor-to-normal tissue signal contrast, long-term retention in tumor and low systemic toxicity. In addition, SA-pNIR effectively converts NIR light into cytotoxic heat in cells, suggesting tumor-activatable photothermal therapy. With the high performance tumor illumination and lysosome-activatable photothermal property, SA-pNIR is a promising agent for detection and photothermal ablation of surgically exposed tumors.

Introduction

With the increasing morbidity and mortality imposed by cancers, approaches that could improve the outcome of existing treatment modalities are of significance.[1] Surgical resection is a mainstay for solid tumor treatment whereupon residual tumors due to incomplete resection often result in tumor relapse. The utility of fluorescence guided surgery is demonstrated by recent clinical treatment of ovarian cancer with the aide of fluorescein-conjugated folate.[2] Recently, optical agents that could direct surgeons to tumor foci evasive to visual inspection are being intensively explored.[2-3]

High tumor-to-background signal contrast is paramount for tumor imaging. As such, optical probes that could be activated to "signal-on" state within tumors while remain silent in off-target settings are critical to achieve low background signals.[3-4] Rhodamine derivatives with intramolecular spirorings are poised to proton triggered fluorogenic opening of the intramolecular rings within acidic lysosomes, enabling high performance tumor imaging in mice models.[5] Relative to rhodamines, near-infrared (NIR) dyes are advantageous for *in vivo* imaging as biological tissues display the least optical absorption and autofluorescence in NIR window (650-900 nm).[6] Nanomaterials that could convert NIR irradiation into cytotoxic heat are being actively explored for photothermal cancer therapy.[7] Given the concerns on biosafety of nanomaterials, small molecular NIR dyes could be biocompatible. For instance, indocyanine green (ICG) has been approved for clinical applications.[8] Analogous to acid-responsive rhodamines, probes display lysosomal acidity activatable NIR fluorescence and photothermal properties have been largely unexplored for intraoperative tumor therapy.

To achieve high tumor-to-background signal contrast required for *in vivo* tumor imaging, dyes are often deliberately armed with tumor-homing entities, such as monoclonal antibody, folate, and aptamers, *etc*.[9] Sialic acids (SA) are anionic monosaccharides commonly located at termini of cell surface glycans,[10] and hypersialylation of cell surface consituents has been identified in a broad spectrum of cancers, [11] suggesting enhanced metabolic demand of SA by these tumors cells. Fluorescein isothiocyanate-labelled sialic acid (SA-FITC) was recently employed for high performance tumor detection in mice, showing effective uptake of SA monosaccharide by metabolically active tumor cells.[12] Albeit selectively accumulated in tumors, SA-FITC suffers from "always-on" green fluorescence which is of limited tissue penetration, and quick *in vivo* clearance which might lead to quick attenuation of tumor-associated signals during surgery.[12] Herein we report a sialylated pH activatable NIR profluorophore (SA-pNIR) for targeted tumor imaging and photothermal therapy in mice with dramatically improved pharmacokinetics critical for clinical translation. SA-pNIR consists of a sialic acid entity for effective *in vivo* tumor uptake and an activatable NIR profluorophore which becomes photothermal and fluorescent within acidic lysosomes.

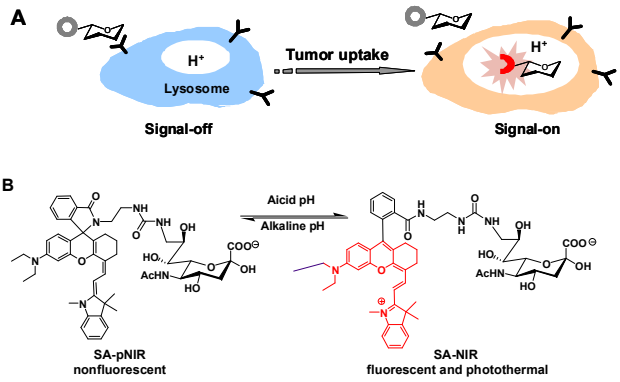

Fig. 1 Schematic of tumor illumination with a targetable sialic acid-conjugated NIR profluorophore (SA-pNIR) activatable to lysosomal acidity (A); nonfluorescent SA-pNIR undergoes acidic pH mediated fluorogenic opening of the intramolecular lactam to give fluorescent and photothermal SA-NIR (B).

Results and discussion

Acidic pH mediated fluorescence activation of SA-pNIR

Optical probes, with turn-on fluorescence inside tumors while

being silent in off-target settings, are beneficial for low-background tumor imaging.[3-4] We recently reported the use of rhodamines with intramolecular spirorings for *in vivo* tumor detection via lysosomal acidity triggered fluorogenic opening of the rings to give rhodamines.[5] Relative to red-emissive rhodamines, NIR dyes are advantageous for bioimaging due to enhanced tissue penetration of NIR fluorescence and the minimal light absorption and autofluorescence of biological tissues in NIR region.[6] Hence, we set to develop a NIR probe, akin to rhodamine-lactams, for tumor imaging *via* lysosomal acidity-mediated fluorescence activation within tumors (Fig. 1B).

((E)-2-(2-(9-(2-carboxyphenyl)-6-(diethyl-amino)-2,3-dihydro-1H-xanthen-4-yl)vinyl)-1,3,3-trimethyl-3H-indol-1-ium perchlorate), a NIR dye reported by Lin *et al,*[13] was first amidated with ethylenediamine and then conjugated with 9-amino-9-deoxy-5-*N*-acetylneuraminic acid to afford desired SA-pNIR in 32% overall yield (ESI†). To probe its pH responsiveness, SA-pNIR was spiked into buffers of pH 4.0-8.0 and the fluorescence emission and UV-vis-NIR absorption of the solutions were recorded over buffer pH. As shown in Fig. 2, SA-pNIR exhibits NIR absorption and fluorescence emission in acidic media, proving proton mediated isomerization of SA-pNIR into fluorescent SA-NIR as described in Fig. 1B. pH titration shows that SA-pNIR is weakly fluorescent at cytosolic pH (pH 7.2) and yet enhanced fluorescence at pH 4.5-6.0 which ideally matches the lysosomal pH window (pH 4-6). These results indicate the applicability of SA-pNIR to illuminate acidic lysosomes in living cells.

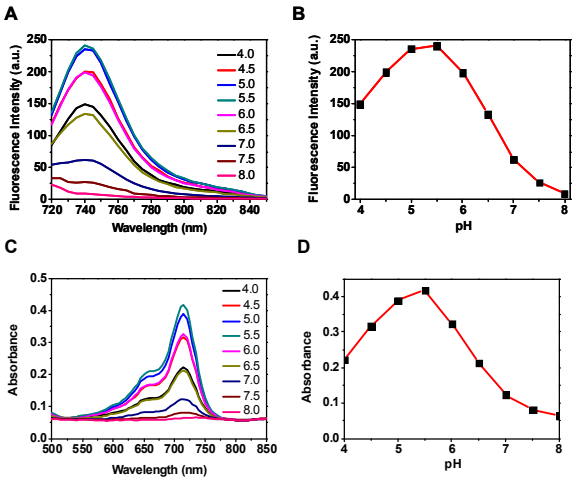

Fig. 2 pH responsiveness of SA-pNIR. SA-pNIR was spiked into sodium phosphate buffer (100 mM, pH 4.0-8.0) containing 10% acetonitrile (v/v) to a final concentration of 10 μM. Fluorescence emission of the solutions was recorded using λex@715 nm (A) and the fluorescence intensities@740 nm were plotted over buffer pH (B). UV-vis-NIR absorption spectra of the solutions were collected over buffer pH (C) and the absorbance@715 nm was plotted as a function of buffer pH (D).

Illumination of acidic lysosomes in cells by SA-pNIR

Lysosomes are the major intracellular acidic compartments and the number and acidity of lysosomes could be significantly boosted in cancer cells.[14] To determine the performance of intracellular signal activation, HeLa cells, U87-MG cells and Raw 264.7 cells were respectively cultured in Dulbecco's Modified Eagle's Medium (DMEM) supplemented with SA-pNIR and then stained with LysoTracker Green DND-26 referenced to as Lysotracker green. Confocal microscopic images shows that NIR fluorescence is clearly observed within all the three cell lines tested and colocalizes with Lysotracker green specific for acidic lysosomes (Fig. 3). The colocalization validates that SA-pNIR could be taken up by these cells and then activated to fluorescent SA-NIR within lysosomes. To probe cellular uptake kinetics, HeLa, U87-MG and Raw 264.7 cells were respectively loaded with SA-pNIR and then stained with DiI specific for plasma membrane. The intracellular NIR signals were determined after 1 h, 4 h and 24 h incubation. It was revealed that the intracellular NIR fluorescence intensified upon elongated incubation (Fig. S1, ESI†), suggesting continuous uptake of SA-pNIR from surrounding medium by these cell lines.

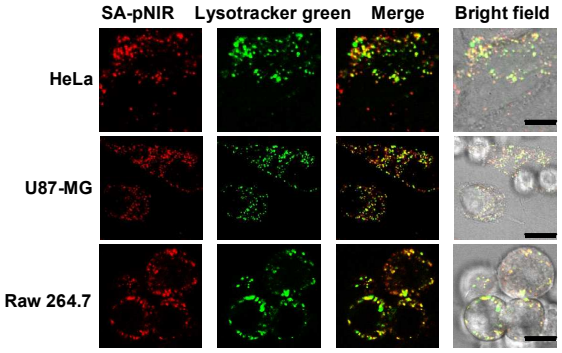

Fig. 3 Lysosome illumination with SA-pNIR. HeLa, U87-MG and Raw 264.7 cells were respectively cultured for 1 h with SA-pNIR (100 μM) in DMEM and then stained with Lysotracker green (1 μM) for 20 min. The cells were probed by confocal fluorescence microscopy. Merging of SA-NIR signal (shown in red) and that of Lysotracker green (shown in green) revealed colocalization, as indicated by the yellow areas. Bars, 10 μm.

To assess the dependence of intracellular NIR fluorescence on lysosomal acidity, we acquired SA-pNIR signals in cells treated with Bafilomycin A1 (BFA), which is a potent inhibitor of V-ATPase and effectively alkalinizes lysosomes in BFA-treated cells.[15] As shown in Fig. 4, the intracellular signals of SA-pNIR largely vanished in HeLa, U87-MG and Raw 264.7 cells pretreated with BFA compared to the cells in the absence of BFA. The BFA- and SA-pNIR treated cells that displayed marked decreased NIR signals within cells were further incubated in phosphate buffer of pH 4.0. Fig. 4 revealed recovered intense intracellular NIR signals in the aforementioned HeLa, U87-MG and Raw 264.7 cells in acidic buffer, excluding the loss of intracellular SA-pNIR in BFA-treated cells and further confirming lysosomal pH dependent "turn-on" fluorescence of Sa-pNIR in cells. Solid tumors are hallmarked by acidic microenvironment due to metabolically accumulated lactic acid.[16] The acidic microenvironment has been widely targeted for tumor therapy and imaging. The recovered NIR fluorescence of BFA-treated cells in acidic buffer strongly indicates that the acidic tumor microenvironments and tumor lysosomes might exert synergistic effects on signal activation of SA-pNIR endocytosed into tumor cells *in vivo*.

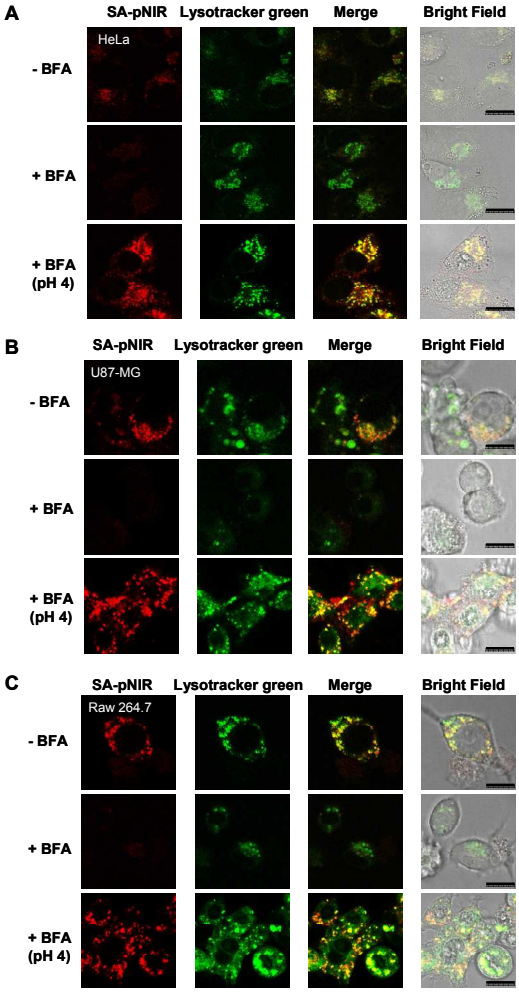

Fig. 4 Acidic pH mediated fluorescence-on of SA-pNIR within cells. HeLa (A), U87-MG (B) and Raw 264.7 (C) cells pretreated with or without BFA (50 nM) were respectively cultured with SA-pNIR (100 μM) in DMEM for 1 h and then stained with Lysotracker green (1 μM) in DMEM for 20 min. For control experiment, cells loaded with BFA and SA-pNIR were resuspended in sodium phosphate buffer (pH 4, 100 mM) for 10 min. The cells were visualized by confocal fluorescence microscopy. The intracellular NIR signals were merged with Lysotracker green and the colocalization is shown by the yellow areas. Bars, 10 μm.

Illumination of subcutaneous tumors in mice with SA-pNIR

Shown to fluoresce in lysosomes, SA-pNIR was further evaluated for its efficacy and selectivity to illuminate subcutaneous tumors in mice. Nude or ICR mice were inoculated subcutaneously with H22 hepatocellular carcinoma cells and then maintained for 5-10 days to allow the development of tumor xenografts. SA-pNIR were intravenously administered into the tumor-bearing nude mice *via* tail vein. The mice were imaged for whole body NIR fluorescence over the course of 144 h after injection. No NIR signal was observed in mice 30 min after administration (Fig. 5), demonstrating that SA-pNIR remained silent during circulation in blood stream (pH 7.4). Intense NIR fluorescence was identified in subcutaneous tumor at 48 h postinjection and the signal contrast between tumor and normal tissues remains high up to 144 h postinjection (Fig. 5). The tumor associated fluorescence validates that SA-pNIR is effectively accumulated in tumor where it is activated to "signal-on" state.

To further determine the biodistribution of SA-pNIR in subcutaneous tumor and healthy tissues, the tumor and representative organs were dissected from tumor-bearing ICR mice pretreated with SA-pNIR for 48 h and then probed by *ex vivo* fluorescence analysis. Consistently, intense signals were observed in tumor whereas moderate to low levels of NIR fluorescence were present in kidney, heart, spleen, lung and liver (Fig. 6B), validating effective tumor uptake and activation of SA-pNIR within tumor. The liver- and kidney-associated NIR fluorescence suggests renal and hepatic clearance of injected SA-pNIR, which is beneficial for clinical translation. Collectively, these data confirm preferential *in vivo* tumoral uptake of SA-pNIR and ensuing fluorescence activation of SA-pNIR, which correlate well with the aforementioned whole body imaging studies (Fig. 5).

In previous tumor imaging studies, the fluorescence of SA-FITC within tumors reached maxima at 20 min post-inection and then quickly decreased by 80% at 1 h postinjection.[12] The long-term retention of SA-pNIR within tumors together with the preferential tumor accumulation of SA-pNIR and the high tumor-to-healthy tissue signal ratios, and suggests the potential utility of SA-pNIR for low background intraoperative tumor detection.

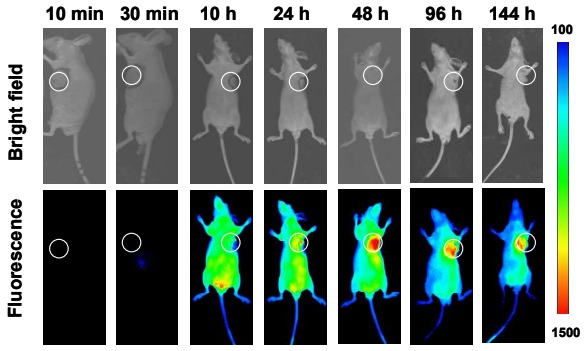

Fig. 5 Time elapsed illumination of subcutaneous tumors with SA-pNIR. Nude mice bearing subcutaneous tumors were intravenously injected with SA-pNIR (40 mg kg^{-1}) *via* tail vein and then imaged for *in vivo* NIR fluorescence emission at indicated time points.

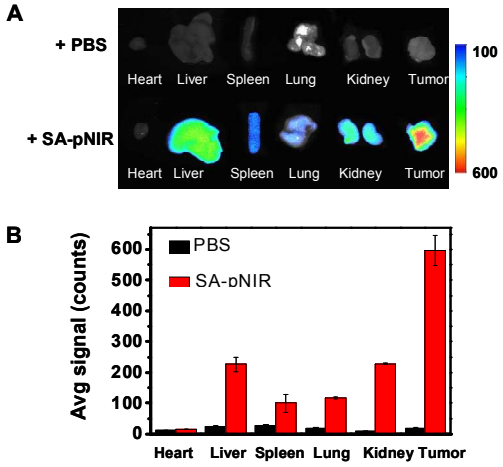

Fig. 6 Biodistribution of SA-pNIR in tumor-bearing mice. ICR mice bearing subcutaneous tumor were intravenously injected with SA-pNIR (40 mg kg^{-1}) or PBS (100 μl) and then sacrificed

48 h postinjection. The tumor and representative organs were dissected and then imaged for *ex vivo* fluorescence emission (A). The bar graph shows the tissue specific NIR fluorescence intensity (B).

To probe the impact of the sialic acid domain of SA-pNIR on *in vivo* tumor targeting, D-glucosamine conjugated with the NIR profluorophore (Glu-pNIR) was prepared and then administered into tumor-bearing ICR mice *via* tail vail (ESI†). In contrast with mice treated with SA-pNIR, whole body imaging revealed no significant NIR signal in subcutaneous tumors from mice treated with Glu-pNIR at 48 and 144 h postinjection (Fig. 7, and Fig. S3, ESI†), demonstrating the critical role of sialic acid for tumor targeting. Historically, monoclonal antibody, folate, peptides, and aptamers have been often used to direct dyes to target tumor.[9] The demonstrated high performance tumor illumination with SA-pNIR shows that sialic acid with C-9 conjugated theranostic entity is an attractive warhead for targetable cancer imaging.

Hypersialylation of cell surface glycoconjugates is a hallmark of a broad spectrum of cancers[11] and often correlates with their metastatic potentials.[17] The tumor-associated over-sialylation suggests enhanced metabolic demands of SA by tumors. Historically, metabolic engineering of cell surface sialosides has been achieved with exogenous *N*-acyl mannosamines, the metabolic precursor of SA.[18] However, this approach is limited by low cell type- or tissue- specificity as demonstrated by broad expression of metabolically synthesized SA in different tissues from supplemented *N*-acyl mannosamines in animals.[19] In contrast, SA-FITC displays high tendency to recognize liver tumors in mice.[12] Albeit preferentially and quickly accumulating in tumors in mice, SA-FITC is poised to quick *in vivo* clearance, leading to significant fluorescence off within tumors. The distinct biomedical properties of SA-pNIR over SA-FITC, *e.g.* long-term tumoral retention, clearly demonstrate the beneficial impacts of pNIR moiety on *in vivo* tumor illumination. These observations reveal that *in vivo* pharmacokinetics of sialic acid-conjugated theranostics could be effectively modulated with substitution of appropriate hydrophobicity (i. e. pNIR vs FITC) at C-9 position of sialic acid.

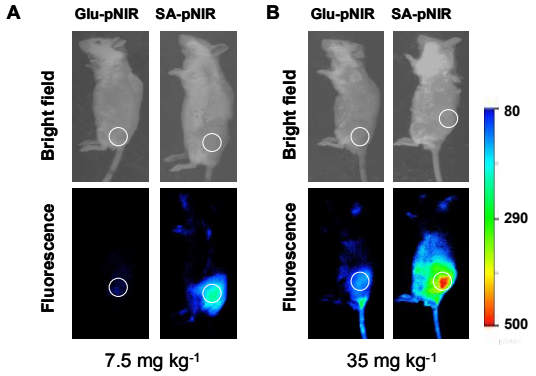

Fig. 7 Sialic acid-mediated tumoral accumulation of SA-pNIR in mice. Tumor-bearing ICR mice were intravenously injected with SA-pNIR or Glu-pNIR with the doses of 7.5 mg kg^{-1} (A) or 35 mg kg^{-1} (B) and then imaged 48 h postinjection.

Cytotoxicity of SA-pNIR

Low toxicity is a prerequisite for imaging agents aimed for *in vivo* administration. We first examined the impacts of SA-pNIR on the survival of HeLa cells by Trypan Blue exclusion test. No obvious detrimental effects on cell viability were observed on cells treated with SA-pNIR for 24 h at doses up to 100 μg ml^{-1} (Fig. 8), suggesting low cytotoxicity that SA-pNIR. To probe the systemic toxicity, SA-pNIR was injected into healthy mice by tail vein at doses of 150 mg kg^{-1}. The mice were regularly monitored for adverse effects following injections. No signs of abnormality, including death, pain and fatigue, were observed on the probe-treated mice up to 10 days after injection. *Ex vivo* analysis revealed low levels of NIR fluorescence in the organs excised from the mice (ESI†, Fig. S5 and S6), suggesting that SA-pNIR could be effectively cleared from the body. Taken together, these results suggest that SA-pNIR is of low biotoxicity.

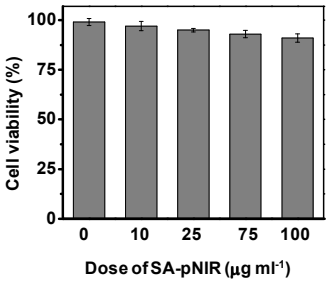

Fig. 8 Cytotoxicity of SA-pNIR. HeLa cells were cultured in DMEM containing various levels of SA-pNIR (0-100 μg ml^{-1}) for 24 h. Cell number and cell viability were determined by trypan blue exclusion assay.

Acidic pH dependent photothermal effects of SA-pNIR

Reagents that could convert optical energy into cytotoxic heat are attractive tools for light-mediated photothermal tumor therapy.[7] As such intense investigations have been devoted to the development of various NIR-absorbing nanomaterials.[7] Given the long-lasting concerns on *in vivo* biosafety of nanoscaled materials, small molecule theranostics are suitable for *in vivo* studies, as demonstrated by the approval of indocyanine green dye (ICG) for clinical applications. Inspired by the emerging use of NIR dyes in photothermal therapy,[20] we proceeded to examine the capability of SA-pNIR as pH-responsive photothermal agents. SA-pNIR was respectively spiked into buffers of pH 7.5 and 4.5. The solutions were exposed to 660-nm laser illumination at the power density of 0.5 W cm^{-2} and the temperature of the solutions was monitored over irradiation time. Fig. 9 clearly shows temperature elevation dependent on the acidic pH, demonstrating that SA-pNIR effectively converts NIR irradiation into heat at acidic media.

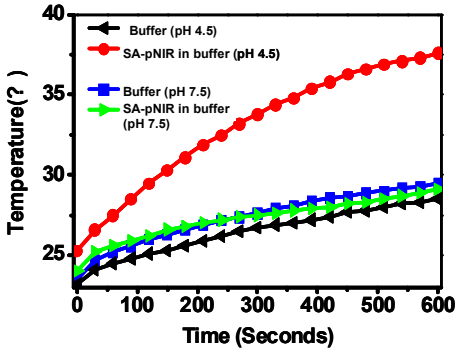

Fig. 9 Acidic pH-dependent photothermal property of SA-pNIR. The temperature of sodium phosphate buffer (100 mM, pH 4.5 or 7.5) containing SA-pNIR (0 or 0.1 mg ml^{-1}) was recorded over the time of irradiation with NIR laser (660 nm, 0.5 W cm^{-2}).

SA-pNIR mediated photothermal killing of cells

SA-pNIR was then evaluated for its photothermal effects on host cells. HeLa, U87-MG and Raw 264.7 cells pre-loaded with SA-pNIR or SA were respectively irradiated with or without NIR laser. Viability of these cell populations was assayed using 3-(4,5-dimethylthiazol-2-yl)-2,5-diphenyltetrazolium (MTT). Cells treated with SA-pNIR and light illumination display further decreased viability relative to that of cells treated with NIR laser or SA-pNIR alone (Fig. 10), demonstrating the synergistic effects of SA-pNIR and light irradiation for detrimental effects on host cells. SA-pNIR is of maximal absorption at 715 nm (Fig. 1). The molecular extinction coefficient at 715 nm is 2-fold higher than that at 660 nm. Given the suboptimal wavelength used photothermal evaluation of SA-pNIR (660 nm, Fig. 9 and Fig. 10), It is anticipatable that the efficacy of SA-pNIR mediated photothermal killing of tumor cells could be further increased with appropriate instrumental laser (715 nm).

Complete manual cytoreduction of small-sized or embedded tumor foci are often challenging during surgery. Photothermal tumor ablation during surgery is applicable due to surgical exposure of cancerous tissues that are otherwise inaccessible to exogenous laser irradiation. Theranostics allowing intraoperative tumor staging and simultaneous photothermal tumor therapy are of clinical significance to complement surgical dissection. The lysosomal acidity-triggered photothermal effect of SA-pNIR on targeted cells supports the potential utility of SA-pNIR as theranostic probe for dual imaging and photothermal killing of tumor foci in intraoperative settings.

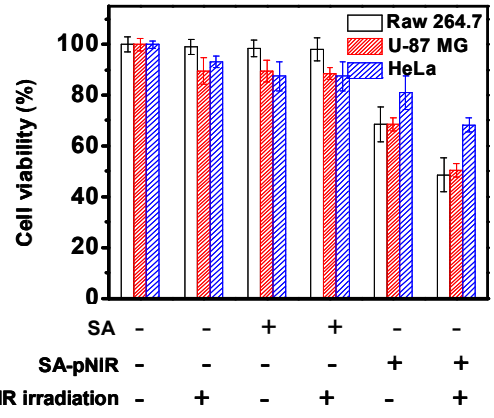

Fig. 10 Photothermal effects SA-pNIR on live cells. HeLa, U87-MG and Raw 264.7 cells were respectively cultured for 24 h with SA-pNIR (0 or 100 μg ml^{-1}) or SA (0 or 100 μg ml^{-1}) in DMEM and then irradiated with or without NIR laser (660 nm, 0.5 W cm^{-2}) in fresh DMEM for 10 min and then further cultured for 24 h. Cell viability were determined by MTT assay.

Conclusions

SA-pNIR, a sialylated lysosome-activatable NIR dye, is developed for intraoperative tumor therapy. The sialic acid entity enables effective tumor-targeting in mice and the NIR profluorophore undergoes lysosomal pH triggered isomerization to give NIR signal. In contrast with SA-FITC which is compromised by "always-on" green fluorescence and quick *in vivo* clearance, SA-pNIR displays signal activation in viable tumor cells, high tumor-to-normal tissue signal contrasts, and long-term retention in tumors, rendering optical imaging over an adequate duration which is critical for practical surgical intervention. In addition, SA-pNIR effectively converts NIR irradiation into heat in acidic lysosomes and leads to obvious cell death upon NIR irradiation, suggesting its utility for photothermal ablation of surgically exposed tumor foci that are otherwise inaccessible to exogenous light. With the superior in vivo pharmacokinetics, high performance tumor illumination, and acid responsive photothermal property, SA-pNIR is a promising small molecular theranostics for fluorescence guided tumor detection and possibly photothermal tumor therapy in intraoperative settings.

Notes and references

[a]*Department of Chemical Biology, College of Chemistry and Chemical Engineering, the Key Laboratory for Chemical Biology of Fujian Province, The MOE Key Laboratory of Spectrochemical Analysis & Instrumentation, and Innovation Center for Cell Biology, Xiamen University;* [b]*State key Laboratory of Cellular Stress Biology, Innovation Center for Cell Biology, School of Life Sciences, Xiamen University, Xiamen, 361005, China; Tel: 86-0592-2181728; E-mail: shoufa@xmu.edu.cn*

Acknowledgments: Dr. S. Han was supported by grants from 973 program 2013CB93390, NSF China (21272196), PCSIRT, and the Fundamental Research Funds for the Central Universities (2011121020); Dr. J. Han was supported by grants from NSF China (30830092, 30921005, 91029304, 81061160512).

† Electronic Supplementary Information (ESI) available on all experimental procedures; synthesis and characterization of SA-pNIR and Glu-pNIR; time course studie son cellular uptake of SA-pNIR; Metabolic incorporation of SA-pNIR into cellular proteins; and whole body images of mice with overdosed SA-pNIR and Glu-pNIR; See DOI: 10.1039/b000000x/

1 Q. T. Nguyen, R. Y. Tsien, *Nat. Rev. Cancer,* 2013, **13**, 653.

2 G. M. van Dam, G. Themelis, L. M. Crane, N. J. Harlaar, R. G. Pleijhuis, W. Kelder, A. Sarantopoulos, J. S. de Jong, H. J. Arts, A. G. van der Zee, J. Bart, P. S. Low, V. Ntziachristos, *Nat. Med.,* 2011, **17**, 1315.

3 (a) H. Lee, W. Akers, K. Bhushan, S. Bloch, G. Sudlow, R. Tang, S. Achilefu, *Bioconjug. Chem.,* 2011, **22**, 777; (b) S. Kumar, R. Richards-Kortum, *Nanomedicine,* 2006, **1**, 23; (c) Y. Urano, D. Asanuma, Y. Hama, Y. Koyama, T. Barrett, M. Kamiya, T. Nagano, T. Watanabe, A. Hasegawa, P. L. Choyke, H. Kobayashi, *Nat. Med.,* 2009, **15**, 104; (d) Q. T. Nguyen, E. S. Olson, T. A. Aguilera, T. Jiang, M. Scadeng, L. G. Ellies, R. Y. Tsien, *Proc. Natl. Acad. Sci. USA.,* 2010, **107**, 4317; (e) Y. Urano, M. Sakabe, N. Kosaka, M. Ogawa, M. Mitsunaga, D. Asanuma, M. Kamiya, M. R. Young, T. Nagano, P. L. Choyke, H. Kobayashi, *Sci. Transl. Med.,* 2011, **3**, 110ra119.

4 (a) H. Kobayashi, P. L. Choyke, *Acc. Chem. Res*., 2011, **44**, 83; (b) H. Kobayashi, M. Ogawa, R. Alford, P. L. Choyke, Y. Urano, *Chem. Rev*., 2010, **110**, 2620.

5 (a) X. Wu, Y. Tian, M. Yu, J. Han, S. Han, *Biomater. Sci*., 2014, **2**, 972; (b) Z. Li, Y. Song, Y. Yang, L. Yang, X. Huang, J. Han, S. Han, *Chem. Sci*., 2012, **3**, 2941.

6 R. Weissleder, V. Ntziachristos, *Nat. Med*., 2003, **9**, 123.

7 (a) E. B. Dickerson, E. C. Dreaden, X. Huang, I. H. El-Sayed, H. Chu, S. Pushpanketh, J. F. McDonald, M. A. El-Sayed, *Cancer Lett*., 2008, **269**, 57; (b) X. Huang, I. H. El-Sayed, W. Qian, M. A. El-Sayed, *J. Am. Chem. Soc*., 2006, **128**, 2115; (c) L. R. Hirsch, R. J. Stafford, J. A. Bankson, S. R. Sershen, B. Rivera, R. E. Price, J. D. Hazle, N. J. Halas, J. L. West, *Proc. Natl. Acad. Sci. USA*., 2003, **100**, 13549; (d) R. Chen, X. Zheng, H. Qian, X. Wang, J. Wang and X. Jiang, *Biomater. Sci*, 2013, **1**, 285

8 J. Malicka, I. Gryczynski, C. D. Geddes, J. R. Lakowicz, *Biomed. Opt*., 2003, **8**, 472e478.

9 (a) P. S. Low, W. A. Henne, D. D. Doorneweerd, *Acc. Chem. Res*., 2008, **41**, 120; (b) M. Schottelius, B. Laufer, H. Kessler, H. J. Wester, *Acc. Chem. Res*., 2009, **42**, 969; (c) O. C. Farokhzad, J. M. Karp, R. Langer, *Expert Opin. Drug Deliv*., 2006, **3**, 311; (d) H. Xu, K. Baidoo, A. J. Gunn, C. A. Boswell, D. E. Milenic, P. L. Choyke, M. W. Brechbiel, *J. Med. Chem*., 2007, **50**, 4759.

10 T. Angata, A. Varki, *Chem. Rev*., 2002, **102**, 439.

11 (a) S. Hakomori, *Cancer Res*., 1996, **56**, 5309; (b) R. Kannagi, K. Sakuma, K. Miyazaki, K. T. Lim, A. Yusa, J. Yin, M. Izawa, *Cancer Sci*., 2010, **101**, 586; (c) Y. Xu, A. Sette, J. Sidney, S. J. Gendler, A. Franco, *Immunol. Cell Biol*., 2005, **83**, 440.

12 X. Wu, Y. Tian, M. Yu, B. Lin, J. Han, S. Han, *Biomater. Sci*., 2014, **2**, 1120.

13 L. Yuan, W. Lin, Y. Yang, H. Chen, *J. Am. Chem. Soc*., 2012, **134**, 1200.

14 G. Kroemer, M. Jaattela, *Nat. Rev. Cancer*, 2005, **5**, 886.

15 T. Yoshimori, A. Yamamoto, Y. Moriyama, M. Futai, Y. Tashiro, *J. Biol. Chem*., 1991, **266**, 17707.

16 R. A. Gatenby, R. J. Gillies, *Nat. Rev. Cancer,* 2004, **4**, 891.

17 (a) R. J. Bernacki, U. Kim, *Science,* 1977, **195**, 577; (b) J. Dennis, C. Waller, R. Timpl, V. Schirrmacher, *Nature,* 1982, **300**, 274.

18 (a) S. J. Luchansky, S. Goon, C. R. Bertozzi, *Chembiochem*., 2004, **5**, 371; (b) C. Oetke, R. Brossmer, L. R. Mantey, S. Hinderlich, R. Isecke, W. Reutter, O. T. Keppler, M. Pawlita, *J. Biol. Chem*., 2002, **277**, 6688; (c) C. Oetke, S. Hinderlich, R. Brossmer, W. Reutter, M. Pawlita, O. T. Keppler, *Eur. J. Biochem*., 2001, **268**, 4553; (d) L. K. Mahal, K. J. Yarema, C. R. Bertozzi, *Science,* 1997, **276**, 1125; (e) E. Saxon, C. R. Bertozzi, *Science,* 2000, **287**, 2007; (f) A. Varki, *FASEB. J*., 1991, **5**, 226.

19 (a) H. Kayser, R. Zeitler, C. Kannicht, D. Grunow, R. Nuck, W. Reutter, *J. Biol. Chem*., 1992, **267**, 16934; (b) J. A. Prescher, D. H. Dube, C. R. Bertozzi, *Nature,* 2004, **430**, 873; (c) A. A. Neves, H. Stockmann, R. R. Harmston, H. J. Pryor, I. S. Alam, H. Ireland-Zecchini, D. Y. Lewis, S. K. Lyons, F. J. Leeper, K. M. Brindle, *FASEB. J*., 2011, **25**, 2528.

20 M. Zheng, C. Yue, Y. Ma, P. Gong, P. Zhao, C. Zheng, Z. Sheng, P. Zhang, Z. Wang, L. Cai, *ACS. Nano*., 2013, **7**, 2056.